



UvA-DARE (Digital Academic Repository)

Combined effects of CO₂ and nitrogen on the stoichiometry of toxin synthesis in a harmful cyanobacterium

Sarkis, Savannah; Liu, Jing; Huisman, Jef; John, Uwe; Verspagen, Jolanda M.H.; Van de Waal, Dedmer B.

DOI

[10.1016/j.hal.2025.102964](https://doi.org/10.1016/j.hal.2025.102964)

Publication date

2025

Document Version

Final published version

Published in

Harmful Algae

License

CC BY

[Link to publication](#)

Citation for published version (APA):

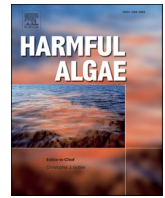
Sarkis, S., Liu, J., Huisman, J., John, U., Verspagen, J. M. H., & Van de Waal, D. B. (2025). Combined effects of CO₂ and nitrogen on the stoichiometry of toxin synthesis in a harmful cyanobacterium. *Harmful Algae*, 150, Article 102964. <https://doi.org/10.1016/j.hal.2025.102964>

General rights

It is not permitted to download or to forward/distribute the text or part of it without the consent of the author(s) and/or copyright holder(s), other than for strictly personal, individual use, unless the work is under an open content license (like Creative Commons).

Disclaimer/Complaints regulations

If you believe that digital publication of certain material infringes any of your rights or (privacy) interests, please let the Library know, stating your reasons. In case of a legitimate complaint, the Library will make the material inaccessible and/or remove it from the website. Please Ask the Library: <https://uba.uva.nl/en/contact>, or a letter to: Library of the University of Amsterdam, Secretariat, P.O. Box 19185, 1000 GD Amsterdam, The Netherlands. You will be contacted as soon as possible.
UvA-DARE is a service provided by the library of the University of Amsterdam (<https://dare.uva.nl>)



Combined effects of CO₂ and nitrogen on the stoichiometry of toxin synthesis in a harmful cyanobacterium

Savannah Sarkis^{a,b,*}, Jing Liu^a, Jef Huisman^b, Uwe John^{c,d}, Jolanda M.H. Verspagen^b, Dedmer B. Van de Waal^{a,b}

^a Department of Aquatic Ecology, Netherlands Institute of Ecology (NIOO-KNAW), PO Box 50, 6700 AB Wageningen, The Netherlands

^b Department of Freshwater and Marine Ecology, Institute for Biodiversity and Ecosystem Dynamics (IBED), University of Amsterdam, PO Box 94240, 1090 GE Amsterdam, The Netherlands

^c Alfred Wegener Institute Helmholtz Centre for Polar and Marine Research, Am Handelshafen 12, 27570 Bremerhaven, Germany

^d Helmholtz Institute for Functional Marine Biodiversity at the University of Oldenburg (HIFMB), Im Technologiepark 5, 26129 Oldenburg, Germany

ARTICLE INFO

Keywords:

Climate change
Harmful cyanobacterial blooms
Microcystis aeruginosa
Microcystins
Ecological stoichiometry

ABSTRACT

The increase in frequency and intensity of harmful cyanobacterial blooms in freshwater ecosystems over past decades has been attributed to anthropogenic influence, notably eutrophication and climate change. *Microcystis* is among the most widespread cyanobacterial bloom-forming genera, some strains of which can produce a range of microcystin variants having different toxicities. The synthesis of microcystins (MCs) is closely linked to carbon and nitrogen metabolism as microcystin variants differ in their nitrogen:carbon ratio. Thus, changes in availability of both CO₂ and nitrogen may impact microcystin production and composition. While the separate effects of CO₂ and nitrogen have been documented, their combined effect is less understood. We therefore assessed the effects of a CO₂ gradient at both nitrogen-replete and -deplete conditions on cellular nitrogen and carbon contents, N:C stoichiometry and microcystin synthesis in three *Microcystis aeruginosa* strains. We observed an interactive effect of increasing CO₂ concentrations with nitrogen availability across strains. Specifically, with increasing CO₂ availability, cellular N:C stoichiometry decreased under nitrogen-deplete conditions from 0.14 to 0.07 but increased under nitrogen-replete conditions from 0.11 to 0.17. Although total cellular microcystin content remained largely unaffected by both CO₂ and nitrogen despite shifts in N:C stoichiometry, changes in variant composition were consistent across strains and followed a stoichiometrically predictable pattern. N-rich but less toxic microcystin variants were favored at high cellular N:C ratios (e.g. MC-RR reached up to 44 % of total MC at highest N:C ratios), whereas relatively less N-containing but more toxic variants became more prevalent at low N:C ratios (e.g. MC-LW shifted from 9 % to 36 % of total MC for one of the strains). This study shows that shifts in CO₂ and nitrogen availability affect cellular N:C stoichiometry and alter microcystin composition, which may cause changes in the toxicity of cyanobacterial blooms.

1. Introduction

Harmful cyanobacterial blooms have been an increasing concern in the past decades due to anthropogenic driven changes in the aquatic environment (Paerl and Huisman, 2008; O'Neil et al., 2012). Eutrophication has been a major contributor to the proliferation of cyanobacteria, while blooms are aggravated by climate change (Chorus and Welker, 2021). Cyanobacterial blooms impose a human health risk through their toxins, which consist of a wide range of secondary metabolites that can be toxic to mammals, birds and fish and affect the

recreational use of lakes, and the preparation of drinking water (Harper, 1992; Huisman et al., 2018). The overall toxicity of cyanobacterial blooms is determined by the types and concentration of toxins, both of which can vary substantially during a bloom. These variations are driven by changes in cyanobacterial species composition, population abundances, and toxin synthesis by individual genotypes. For example, *Microcystis* can produce toxins known as microcystins. A *Microcystis* bloom generally consists of a mixture of non-toxic and toxic genotypes, where toxic genotypes exhibit different microcystin profiles (Johansson et al., 2019). Hence, a successive selection of dominant genotypes can

* Corresponding author.

E-mail address: s.sarkis@nioo.knaw.nl (S. Sarkis).

<https://doi.org/10.1016/j.hal.2025.102964>

Received 28 May 2025; Received in revised form 20 August 2025; Accepted 31 August 2025

Available online 4 September 2025

1568-9883/© 2025 The Author(s). Published by Elsevier B.V. This is an open access article under the CC BY license (<http://creativecommons.org/licenses/by/4.0/>).

change the total microcystin concentration and the microcystin composition during cyanobacterial blooms (Kardinaal et al., 2007a).

Microcystin is one of the most widespread classes of cyanobacterial toxins and causes gastroenteritis, damage to the liver, and is likely tumor-promoting (Carmichael, 2001; Zurawell et al., 2005; Meriluoto et al., 2017). A microcystin molecule is a cyclic peptide consisting of seven amino acids, with a variable amino acid composition at positions two and four (Welker and Von Döhren, 2006). This variation in amino acid composition has resulted in more than 270 variants of microcystin (Bouaïcha et al., 2019). The microcystin variants differ in their hydrophobic properties, which affects the toxicity of the molecule, with the more hydrophobic variants being more toxic (Fischer et al., 2010). For instance, microcystin-LR (MC-LR), the most common microcystin, has leucine (L) and arginine (R) at the two variable positions and has an LD₅₀ of 50 µg/kg (based on intraperitoneal injection in mice) (Zurawell et al., 2005). MC-RR contains two arginine (R) molecules and has a relatively high LD₅₀ of ~600 µg/kg, making it one of the least toxic variants, while MC-LW has leucine (L) and tryptophan (W) at these positions and is one of the most toxic variants. No LD₅₀ data are available for this toxin variant, but it has been shown to be cytotoxic to human primary hepatocytes and OATP-transfected human embryonic kidney cells (Fischer et al., 2010).

Microcystins are nitrogen-rich molecules, and thus it can be expected that the production of microcystins depends on the availability of nitrogen (Downing et al., 2005; Gobler et al., 2016). Indeed, the cellular microcystin content was shown to increase with the amino acid and nitrogen contents in the cells (Van de Waal et al., 2010). A positive relationship was also observed between microcystin concentrations and nitrogen availability during blooms (Vézie et al., 2002; Downing et al., 2005; Harke and Gobler, 2015). Overall, the microcystin content of cells is stoichiometrically regulated, and increases with higher cellular nitrogen:phosphorus (N:P) and nitrogen:carbon (N:C) ratios (Wagner et al., 2019; Brandenburg et al., 2020). Interestingly, the various amino acids have different nitrogen requirements, which also leads to different N:C ratios of the microcystin variants. For example, arginine is the nitrogen-richest amino acid, making MC-RR the microcystin variant with the highest N:C ratio of 0.26. In contrast, MC-LW has a relatively low N:C ratio of 0.15. The composition of microcystins has also been shown to follow stoichiometrically predictable patterns. For instance, it has been shown that an increase in the cellular N:C ratio of *Microcystis aeruginosa* at high nitrogen availability was associated with an increase in MC-RR over MC-LR both in laboratory experiments and in the field (Van de Waal et al., 2009). Likewise, a recent field study in Lake Erie showed that microcystin composition was dominated by MC-RR early in the bloom season when dissolved inorganic nitrogen was still available, but shifted towards the less nitrogen-containing but more toxic MC-LA (N:C = 0.15) when nitrogen became limiting later in the season (Chaffin et al., 2023). So, excess nitrogen may result in high overall microcystin concentrations during blooms, while simultaneously favoring the less toxic microcystin variant.

Inorganic carbon is also an essential resource for cyanobacterial blooms. During bloom development, CO₂ is fixed through photosynthesis, which can lead to a depletion of dissolved CO₂ levels down to <10 µatm (Talling, 1976; Maberly, 1996; Balmer and Downing, 2011). Conversely, freshwater lakes can be supersaturated with CO₂ with partial pressures reaching more than 10,000 µatm due to the degradation of organic matter (Cole et al., 1994; Lazzarino et al., 2009; Sandrini et al., 2014). So, the primary producers of the lake, including the bloom-forming cyanobacterial species, may experience an excessive amount of CO₂ before the bloom season, while their growth may become potentially carbon limited during dense blooms (Verspagen et al., 2014a). Cyanobacteria have different carbon concentrating mechanisms (CCMs) that give them the ability to take up both CO₂ and HCO₃⁻ as a carbon source (Price et al., 2004; Sandrini et al., 2014; Ji et al., 2020). Moreover, various *Microcystis* genotypes were shown to have different affinities for CO₂, and changes in CO₂ levels may thus lead to shifts in

population dynamics and the dominance of toxic genotypes (Van de Waal et al., 2011; Sandrini et al., 2014, 2016).

While the impacts of elevated CO₂ levels and nitrogen availability on harmful cyanobacteria have been studied separately, we know little about their potential interactions. We therefore assessed how different concentrations of CO₂ at high and low nitrogen supply affect N:C stoichiometry and microcystin synthesis in three toxic strains of *Microcystis aeruginosa* with different combinations of microcystin variants. Specifically, we tested the following three hypotheses: (1) Increasing pCO₂ will lead to a decrease in cellular N:C ratios, particularly under nitrogen replete conditions. (2) In response to lower cellular N:C ratios, cellular contents of microcystins will also decline as they are nitrogen-rich compounds; this trend will be particularly pronounced under nitrogen deplete conditions. (3) A decrease in N:C ratios driven by increasing pCO₂ and nitrogen limitation will favor synthesis of the less nitrogen-containing (but more toxic) microcystin variants MC-LW, -LY, and -LF, at the cost of the nitrogen-richest (but less toxic) microcystin variant MC-RR.

2. Methods

2.1. Experimental conditions

Three microcystin-producing strains of *Microcystis aeruginosa* were selected: PCC 7820 from the Pasteur Culture Collection, France, NIES 1099 from the Microbial Culture Collection at the National Institute for Environmental Studies, Japan, and HUB 524 from the Humboldt University of Berlin, Germany. The microcystin composition differed between the three strains, but all measured microcystin variants were found in at least two strains, and MC-LR was found in all three strains (Table 1).

The three strains were incubated at five different CO₂ levels in the gas flow (i.e. a pCO₂ of 50, 200, 400, 800, 1600 µatm) in nitrogen replete (N-replete) and nitrogen deplete (N-deplete) treatments, resulting in a total of 30 treatments. For the N-replete treatments, the strains were grown in batch cultures that enable unconstrained growth during the exponential phase. For the N-deplete treatments, the strains were cultured in chemostats and grown to steady state under N-limited conditions. Cultures were grown in monoculture but were not axenic. Continuous aeration with moistened gas at the bottom of the batch and chemostat vessels caused homogeneous mixing, which prevented settling of the cells. Microscopic inspection confirmed that cells were grown generally as single cells. The gas was a mixture of N₂, O₂ and CO₂ for the lower than ambient CO₂ treatments. Higher CO₂ treatments consisted of pressurized air and specific amounts of additional CO₂ gas. The gases were combined using a Brooks® Smart II mass flow controller, which controlled the gas pressure of the components and the mixture. The cells were grown under saturating light conditions, with a light

Table 1

The microcystin variants investigated in this study, the *Microcystis aeruginosa* strains that produce them, the N:C ratios of the microcystin variants, their LD₅₀, and their toxicity factor relative to MC-LR. The toxicity factor was calculated based on the LD₅₀ values on mice as well as EC₅₀ values on primary human hepatocytes and OATP-transfected human embryonic kidney cells (Faassen and Lürding, 2013).

Microcystin variant	Microcystis strains			N:C ratio	LD ₅₀ (µg/kg)	Toxicity factor
	PCC 7820	NIES 1099	HUB 524			
MC-RR	-	Yes	Yes	0.26	500–800	0.08
MC-LR	Yes	Yes	Yes	0.20	50	1
MC-YR	-	Yes	Yes	0.19	150–200	0.29
MC-LW	Yes	Yes	-	0.15	n.a	7
MC-LF	Yes	Yes	-	0.14	n.a	7
MC-LY	Yes	Yes	-	0.14	90	0.56

intensity of $100 \pm 15 \mu\text{mol photons } m^{-2} s^{-1}$ supplied by fluorescent tubes (PL-L 24W/840/4p, Philips) at a light:dark cycle of 16:8 h. The temperature was maintained at $22 \pm 1^\circ\text{C}$.

2.1.1. Carbonate chemistry

Dilute batch experiments (N-replete) as well as chemostat experiments (N-deplete) were performed with the same gas mixture, leading to similar, but not equal CO_2 conditions. The dissolved CO_2 concentration in each culture was calculated based on pH and alkalinity measured on harvest day, taking into account temperature, salinity, dissolved inorganic phosphorus and boric acid concentrations (Text S1), and will be expressed as $p\text{CO}_2(\text{aq})$.

2.1.2. Batch experiments

The three *Microcystis* strains were grown in 1 L bottles, with triplicates for each strain and each $p\text{CO}_2$ treatment. The cultures were grown in modified WC medium (Kilham et al., 1998) leaving out $\text{Na}_2\text{SiO}_3 \cdot 9\text{H}_2\text{O}$ since silicate is not required for cyanobacteria, with an NO_3^- concentration of $1000 \mu\text{mol L}^{-1}$, and HCO_3^- adjusted to $500 \mu\text{mol L}^{-1}$. Before starting the experiments, the batch cultures were acclimated to the experimental conditions of the different $p\text{CO}_2$ treatments (i.e. by growing them in modified WC medium, using the applied $p\text{CO}_2$, temperature and light conditions) for 7–11 days (i.e. around 7 generations), after which the acclimated culture was added to fresh medium at the start of the experiment. Every day, measurements were performed for pH, cell counts, and biovolume. After 4 days (i.e. 2–3 generations) the cells were harvested around the middle of the light period and additional samples were taken for the determination of alkalinity, particulate organic carbon and nitrogen (referred to as organic carbon content or C-content, and organic nitrogen content or N-content respectively), and microcystins.

2.1.3. Chemostat experiments

The three *Microcystis* strains were grown in chemostats in duplicates per $p\text{CO}_2$ treatment. The chemostats had a working volume of 1.7 L and an optical path length of 5 cm (Huisman et al., 2002). The strains were grown in the same medium as used for the batch experiment, but with NO_3^- concentrations reduced to $200 \mu\text{mol L}^{-1}$, and medium was provided at a dilution rate of $0.2 d^{-1}$. The temperature was maintained by a cooling finger. The chemostat cultures were acclimated to the different $p\text{CO}_2$ treatments for a period of 2–3 weeks (i.e. at least 5 generations). Treatments were run until steady-state was reached, defined as the level at which the biovolume stabilized and variation remained within 10 % of the mean for at least a week (i.e. three consecutive measurements). The pH, cell count and biovolume were measured three times a week. Alkalinity was measured on average once a week. At steady-state, samples were taken for dissolved inorganic nitrogen (NO_3^-) to confirm it was the limiting resource. On the final day, around the middle of the light cycle, additional samples were taken for carbon and nitrogen content, and microcystins. After a $p\text{CO}_2$ treatment was finished, >80 % of the volume was removed, chemostat vessels were slowly refilled with fresh medium (at $340 \text{ mL } d^{-1}$), and cultures were acclimated to the next $p\text{CO}_2$ treatment for a period of 2–3 weeks (i.e. at least 5 generations) to prevent carry-over effects from the preceding $p\text{CO}_2$ treatment. For the PCC 7820 at the $p\text{CO}_2$ treatment of $1600 \mu\text{atm}$, one of the replicates washed out (i.e. growth rate dropped below the dilution rate) and only one of the replicates remained. Consequently, for this strain, data is only available for a single chemostat at the highest $p\text{CO}_2$ treatment.

2.2. Measurements

After samples were taken, pH and temperature were measured with a pH electrode (pH/cond 340i, WTW), while the sample was being stirred by a magnetic stirrer. Cell counts and biovolume were measured using a cell counter (Multisizer™ 3 Coulter Counter, Beckman). Samples for alkalinity were filtered over pre-washed GF/F glass microfiber filter

(pore size $\sim 0.7 \mu\text{m}$, Whatman™) and then analyzed (TIM840 titration manager, Titrilab). Samples for nutrients were filtered over a mixed cellulose membrane filter (pore size $0.45 \mu\text{m}$, Satorius), stored at -20°C and afterwards analyzed on a QuAAtro segmented flow Autoanalyzer (Seal Analytical, Beun DeRonde). Organic carbon and nitrogen contents were determined by filtering 10–60 mL of the culture suspension through a demi-water pre-washed 25 mm GF/F filter (Whatman™) to get approximately $10^8 \mu\text{m}^3$ *Microcystis* biovolume on the filter. The filters were dried at 60°C overnight, stored in a desiccator, and then analyzed for carbon and nitrogen on a Thermo NC analyser (Flash 1112, Interscience). Microcystin extraction and measurements were done according to the protocol used in Liu et al. (2016), as outlined below.

2.3. Microcystin measurements

The culture was filtered (15–30 mL) through a 25 mm GF/F filter (Whatman™), and stored at -20°C . Before extraction, filters were freeze-dried for 6 h. The extraction process was repeated three times to ensure maximum extraction of microcystins. The extraction process involved incubating the freeze-dried filters in 2.5 mL of 75 % methanol solution at 60°C for 30 min, followed by centrifuging the extracts, and transferring the supernatant into 8 mL glass collection tubes. After this was repeated a total of three times, the collected extract was evaporated in a Savant™ SPD121P speedvac (Thermo Scientific) at 50°C for 6–8 h. The dried pellet was dissolved in $3 \times 300 \mu\text{L}$ 100 % methanol and filtered through a $0.2 \mu\text{m}$ cellulose-acetate filter (Grace Davison Discovery Science) in an Eppendorf tube by centrifugation for 5 min at $16,000 \times g$ (Galaxy 16DH, VWR™). The filtrate was then transferred to an amber vial and stored at -20°C . Samples were analysed for the microcystin variants [Dhb⁷] MC-RR, MC-RR, [Dhb⁷] MC-LR, MC-LR, MC-YR, MC-LY, MC-LF and MC-LW by liquid chromatography–tandem mass spectrometry (LC-MS/MS) as described in Faassen & Lüring (2013). [Dhb⁷] MC-RR and MC-RR were pooled as MC-RR; [Dhb⁷] MC-LR and MC-LR were pooled as MC-LR. Separation was performed with an Agilent 1200 LC system and an Agilent Zorbax Eclipse XDB-C184.6 \times 150 mm, $5 \mu\text{m}$ column, with water with 0.1 % formic acid and acetonitrile with 0.1 % formic acid as eluents. The Agilent 6410 MS/MS was operated in positive mode with an electrospray ionization source. For each variant, two transitions were monitored in multiple reaction monitoring (MRM) mode. Samples were quantified against a calibration curve in methanol, and standards were obtained from DHI LAB products (Hørsholm, Denmark). We note that we assessed the free methanol-soluble microcystins in our study, while the microcystins that are bound to intracellular compounds are not accounted for (Meissner et al., 2013). Microcystins have been shown to bind to a number of proteins, notably those involved in the Calvin cycle, including RubisCO which is enhanced under high light levels and oxidative stress (Zillig et al., 2011).

2.4. Growth rates

In batch culture, the specific growth rate (μ) during the exponential growth phase equals:

$$\mu = \frac{d(\ln B)}{dt} \quad (1)$$

where B is the biovolume on day t , and t is time in days. Accordingly, the specific growth rate in the N-replete batch cultures was calculated from the slope of a linear regression of $\ln(B)$ vs. time, using either three or four data points depending on the duration of the exponential growth phase.

In steady-state chemostats, the specific growth rate (μ) equals the dilution rate (D) for all cultures (i.e., $\mu = D = 0.2 d^{-1}$). Therefore, the responses to $p\text{CO}_2$ in the different chemostat experiments were independent of changes in growth rate. Furthermore, at steady-state, nitrate consumption equals the supply rate. This allows chemostats with low

nitrate concentrations in the supplied medium to reach and maintain N-limited conditions.

Microcystin synthesis is known to be influenced by cell size and growth rate. We corrected for variations in cell size by normalizing cellular microcystin to biovolume. To also correct for differences in growth rates, we calculated net microcystin production rates by multiplying microcystin content with specific growth rates.

2.5. Statistical analyses

We used an asymptotic regression model for the non-linear relationships of C-content, N-content, cellular N:C ratios, microcystin content and microcystin production with $p\text{CO}_2(\text{aq})$:

$$y = A - (A - B)e^{-Cx} \quad (2)$$

where x is the $p\text{CO}_2(\text{aq})$ in μatm , and y is the response variable (i.e. C-content, N-content, N:C ratio, microcystin content, and microcystin production). Furthermore, A is the asymptotic value of the response variable when $p\text{CO}_2(\text{aq})$ approaches infinity, B is the y-intercept (i.e., the value of the response variable when $p\text{CO}_2(\text{aq})$ equals zero), and C is the rate at which the function approaches the asymptote. The model was used to explain the data whenever A and B were significant ($p < 0.05$), and the confidence interval of y was less than four times the mean for all $p\text{CO}_2$ levels in the regression. When only one of the two parameters, or none, were significant, or when the confidence interval was greater than four times the mean, the mean of the response variable was used instead.

If the $p\text{CO}_2$ responses of both N-treatments were described by an asymptotic regression, the effect of nitrogen availability on the $p\text{CO}_2$ response was tested by comparing the asymptotes and intercepts (i.e., the parameters A and B) of the regression models of the N-replete versus N-deplete treatments. In this case, a Wald test was used to test for significant differences between the parameter estimates:

$$W = \frac{(A_1 - A_2)^2}{\text{Var}(A_1) + \text{Var}(A_2)} \quad (3)$$

where A_1 and A_2 are the asymptotes estimated for the N-replete and N-deplete treatments, respectively, and $\text{Var}(A_1)$ and $\text{Var}(A_2)$ are the variances of these parameter estimates. A similar Wald test was used to test for significant differences between the y-intercepts B_1 and B_2 estimated for the N-replete and N-deplete treatments.

If the $p\text{CO}_2$ response of only one of the N-treatments was described by the asymptotic regression model while the other N-treatment was described by the mean, then a modified Wald test was used (i.e. a Z-test) to test for significant differences between the asymptote (parameter A in

the model) and the mean:

$$Z_A = \frac{A - \text{mean}}{\sqrt{\text{SE}_A^2 + \text{SE}_{\text{mean}}^2}} \quad (4)$$

where SE_A and SE_{mean} are the standard errors of parameter A and the mean, respectively. The Z_A score quantifies the difference between the asymptote and the mean in terms of their combined standard errors. A similar modified Wald test was used to test for significant differences between the y-intercept B and the mean of the two models. For all tests, significant differences between N-treatments were established using a significance level of 0.05.

3. Results

3.1. Carbonate chemistry

The $p\text{CO}_2$ treatments resulted in consistent differences in $p\text{CO}_2(\text{aq})$ in the cultures, ranging from $41 \pm 25 \mu\text{atm}$ to $2917 \pm 131 \mu\text{atm}$ in the N-replete batch cultures and from $5 \pm 3 \mu\text{atm}$ to $1875 \pm 187 \mu\text{atm}$ in the N-deplete chemostats (Table 2, Table S1–2, Fig. S1). The very low $p\text{CO}_2(\text{aq})$ in the chemostat cultures treated with $50 \mu\text{atm}$ of CO_2 in the gas flow is indicative of CO_2 depletion by the photosynthetic activity of the cyanobacteria. In line with expectation, pH values ranged from ~ 7.2 at elevated $p\text{CO}_2$ to high values up to 9.4 when CO_2 in the cultures was depleted. The increase in alkalinity at elevated $p\text{CO}_2(\text{aq})$ can be attributed to the uptake of nutrient anions (e.g., NO_3^- , HPO_4^{2-}) by the cells, which is coupled to the uptake of protons (H^+) for cells to maintain charge balance (Wolf-Gladrow et al., 2007; Verspagen et al. 2014a).

Under N-deplete conditions in the chemostats, steady-state dissolved inorganic nitrogen (DIN) concentrations were relatively high in the lowest $p\text{CO}_2$ treatment of $50 \mu\text{atm}$, but sharply dropped and remained below $5 \mu\text{mol/L}$ in the $p\text{CO}_2$ treatments of $\geq 200 \mu\text{atm}$ (Table S3). These low steady-state DIN concentrations indicate N-limitation in the chemostats with $p\text{CO}_2$ treatments of $\geq 200 \mu\text{atm}$, while at the $p\text{CO}_2$ treatment of $50 \mu\text{atm}$ cultures may have been C-limited and/or co-limited by CO_2 and nitrogen.

3.2. Cellular carbon and nitrogen

Overall, the cellular C-content either remained constant or decreased with increasing $p\text{CO}_2(\text{aq})$ and then levelled off (Fig. 1. A-C, Table S4). Specifically, with increasing $p\text{CO}_2(\text{aq})$, the C-content in the N-replete treatments decreased consistently for all strains. For PCC 7820, the C-content decreased sharply with increasing $p\text{CO}_2(\text{aq})$ until it levelled off at

Table 2

Overview of carbonate chemistry in nitrogen replete (batch) and nitrogen deplete (chemostat) cultures, treated with different partial pressures of CO_2 ($p\text{CO}_2$) in the gas flow; data show $p\text{CO}_2(\text{aq})$, pH, alkalinity and dissolved inorganic carbon (DIC). Values indicate mean \pm SD ($n = 3$ for batch, $n = 2$ for chemostats).

	$p\text{CO}_2$ treatment (μatm)	Nitrogen replete – Batch				Nitrogen deplete – Chemostat			
		$p\text{CO}_2(\text{aq})$ (μatm)	pH	Alkalinity (mEq/L)	DIC (mmol/L)	$p\text{CO}_2(\text{aq})$ (μatm)	pH	Alkalinity (mEq/L)	DIC (mmol/L)
PCC 7820	50	53 ± 19	8.51 ± 0.11	0.55 ± 0.02	0.32 ± 0.03	8 ± 9	9.26 ± 0.26	0.67 ± 0.06	0.26 ± 0.08
	200	141 ± 9	8.20 ± 0.01	0.59 ± 0.03	0.41 ± 0.04	109 ± 11	8.41 ± 0.01	0.70 ± 0.02	0.52 ± 0.03
	400	398 ± 24	7.81 ± 0.01	0.61 ± 0.03	0.48 ± 0.02	317 ± 124	8.08 ± 0.04	0.83 ± 0.15	0.69 ± 0.17
	800	1107 ± 26	7.50 ± 0.01	0.76 ± 0.01	0.69 ± 0.02	1099 ± 11	7.62 ± 0.00	0.93 ± 0.00	0.86 ± 0.01
	1600	2522 ± 203	7.17 ± 0.03	0.78 ± 0.01	0.78 ± 0.02	1809	7.34	0.80	0.78
NIES 1099	50	41 ± 25	8.60 ± 0.19	0.55 ± 0.04	0.29 ± 0.03	5 ± 4	9.37 ± 0.13	0.69 ± 0.02	0.25 ± 0.07
	200	130 ± 14	8.22 ± 0.00	0.56 ± 0.04	0.40 ± 0.05	80 ± 4	8.51 ± 0.02	0.68 ± 0.02	0.48 ± 0.01
	400	411 ± 38	7.81 ± 0.02	0.61 ± 0.01	0.50 ± 0.02	638 ± 22	7.87 ± 0.01	0.98 ± 0.06	0.87 ± 0.06
	800	1091 ± 11	7.55 ± 0.01	0.82 ± 0.01	0.75 ± 0.01	1293 ± 103	7.56 ± 0.01	0.95 ± 0.04	0.89 ± 0.05
	1600	2711 ± 165	7.15 ± 0.03	0.78 ± 0.04	0.81 ± 0.02	1743 ± 83	7.34 ± 0.01	0.78 ± 0.01	0.75 ± 0.02
HUB 524	50	44 ± 35	8.60 ± 0.22	0.57 ± 0.03	0.31 ± 0.06	5 ± 3	9.37 ± 0.12	0.64 ± 0.03	0.22 ± 0.02
	200	132 ± 16	8.20 ± 0.01	0.58 ± 0.04	0.39 ± 0.04	76 ± 9	8.51 ± 0.02	0.66 ± 0.02	0.46 ± 0.02
	400	410 ± 10	7.81 ± 0.01	0.62 ± 0.02	0.50 ± 0.01	577 ± 90	7.88 ± 0.04	0.91 ± 0.00	0.80 ± 0.01
	800	1064 ± 70	7.55 ± 0.01	0.81 ± 0.01	0.73 ± 0.02	1093 ± 39	7.62 ± 0.01	0.92 ± 0.00	0.85 ± 0.00
	1600	2917 ± 131	7.16 ± 0.00	0.85 ± 0.07	0.89 ± 0.05	1875 ± 187	7.29 ± 0.03	0.74 ± 0.00	0.71 ± 0.00

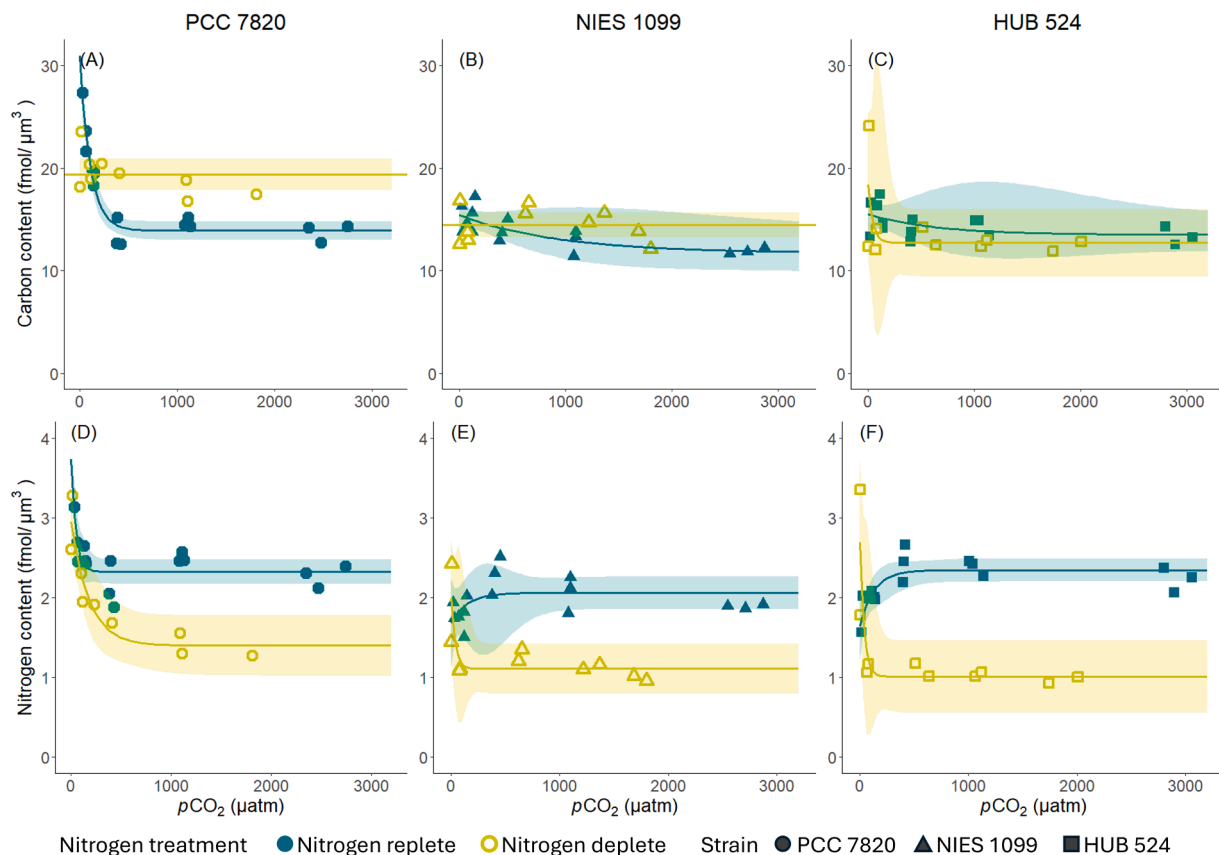


Fig. 1. Carbon (A-C) and nitrogen (D-F) content per biovolume in the N-replete and N-deplete treatments across the $p\text{CO}_2(\text{aq})$ gradient for *Microcystis aeruginosa* strain PCC 7820 (A, D), NIES 1099 (B, E), and HUB 524 (C, F). Lines show the fit of an asymptotic model if two or more of the model parameters were significant ($p < 0.05$) and the confidence interval was less than four times the mean; otherwise, the lines show the mean of all points for the N-replete and N-deplete treatments. The shaded ribbons indicate the 95 % confidence interval of the model.

$\sim 500 \mu\text{atm}$. For NIES 1099 and HUB 524, the C-content decreased more gradually with increasing $p\text{CO}_2(\text{aq})$ and levelled off at $p\text{CO}_2(\text{aq}) \sim 2500 \mu\text{atm}$. Under N-deplete conditions, C-content remained unchanged with increasing $p\text{CO}_2(\text{aq})$ for PCC 7820 and NIES 1099, while it decreased for HUB 524 where it levelled off at a $p\text{CO}_2(\text{aq})$ of $\sim 100 \mu\text{atm}$. C-content did not show a significant difference between the two N-treatments for NIES 1099 and HUB 524 (Table S5). In PCC 7820, the C-content was significantly higher in the N-replete than in the N-deplete treatment at low $p\text{CO}_2(\text{aq})$ (parameter B, Tables S4–5), while it was significantly lower at high $p\text{CO}_2(\text{aq})$ (parameter A, Tables S4–5).

The cellular N-content in the N-replete treatments increased with increasing $p\text{CO}_2(\text{aq})$ and levelled off at $300\text{--}500 \mu\text{atm}$ for NIES 1099 and HUB 524, while for PCC 7820 it decreased with increasing $p\text{CO}_2(\text{aq})$ and levelled off at $\sim 100 \mu\text{atm}$ (Fig. 1. D–F, Table S4). In the N-deplete treatments, cellular N-content consistently decreased with increasing $p\text{CO}_2(\text{aq})$ for all three strains, reaching an asymptote at $\sim 500 \mu\text{atm}$ for PCC 7820 and at $\sim 100 \mu\text{atm}$ for NIES 1099 and HUB 524. At low $p\text{CO}_2(\text{aq})$, N-content was not significantly different across the N-treatments for PCC 7820 and NIES 1099, while it was significantly higher in the N-deplete than in the N-replete treatment for HUB 524 (parameter B,

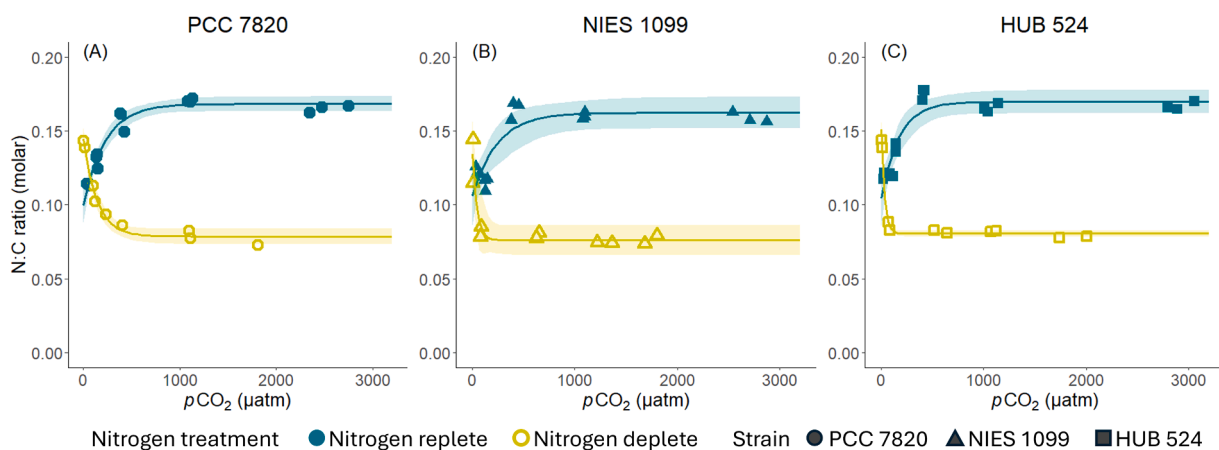


Fig. 2. Cellular N:C ratio in the N-replete and N-deplete treatments across the $p\text{CO}_2(\text{aq})$ gradient for *Microcystis aeruginosa* strain PCC 7820 (A), NIES 1099 (B), and HUB 524 (C). Lines show the fit of an asymptotic model, and shaded ribbons indicate the 95 % confidence interval of the model.

Tables S4–5). At high $p\text{CO}_2(\text{aq})$, N-content was significantly higher in the N-replete treatment than in the N-deplete treatment for all strains (parameter A, Tables S4–5).

The cellular N:C ratios showed an N-dependent trend with increasing $p\text{CO}_2(\text{aq})$ that was consistent across the three strains (Fig. 2). With increasing $p\text{CO}_2(\text{aq})$, the N:C ratios in the N-replete treatments increased toward 0.16–0.17 (parameter A, Table S4). In contrast, the N:C ratios in the N-deplete treatment decreased with increasing $p\text{CO}_2(\text{aq})$ toward 0.07–0.08. At low $p\text{CO}_2(\text{aq})$, all three strains had an intermediate N:C ratio ranging between 0.10–0.15 at both N-treatments.

3.3. Microcystin content, production and composition

The microcystin content was not significantly affected by increasing $p\text{CO}_2(\text{aq})$, nor by the N-treatments (Fig. 3. A–C, Tables S4–5). However, total microcystin production was generally lower in the N-deplete treatments than in the N-replete treatments (Fig. 3. D–F, Tables S4–5), following the cellular N:C ratios which were also lower in the N-deplete treatments than in the N-replete treatments (Fig. 2). Microcystin production did not change significantly with increasing $p\text{CO}_2(\text{aq})$ for the N-deplete treatments across strains, nor for the N-replete treatment for HUB 524. In the N-replete treatments of PCC 7820 and NIES 1099, a significant decrease in microcystin production was observed with increasing $p\text{CO}_2(\text{aq})$ that levelled off at $\sim 1000 \mu\text{atm}$ and $\sim 100 \mu\text{atm}$ respectively. While the effect of the treatments were mostly consistent across strains, the absolute amounts of microcystin content and production were strain specific with PCC 7820 having the highest microcystin content and production, followed by NIES 1099, and then HUB 524. This was shown with a one-way ANOVA with a statistically

significant result for microcystin content ($F(2,71) = 115.8, p < 0.001$) and for microcystin production ($F(2,71) = 32.51, p < 0.001$). A post-hoc TukeyHSD test confirmed that the microcystin content and the microcystin production rate in all three strains differed significantly from each other (Table S6).

The microcystin composition showed marked changes with increasing $p\text{CO}_2(\text{aq})$ that depended on the N availability (Fig. 4, Tables S4–5). With increasing $p\text{CO}_2(\text{aq})$, the fraction of the N-richest (i. e. highest N:C ratio) microcystin variant MC-RR (Fig. 4. A) was significantly higher in the N-replete than the N-deplete treatments (Tables S4–5). In contrast, the fractions of the less N-containing variants, including MC-YR as well as -LW, -LF, and, for NIES 1099, also MC-LY were higher in the N-deplete compared to N-replete treatments (Fig. 4. C–F, Tables S4–5). At low $p\text{CO}_2(\text{aq})$, the effect of nitrogen is less apparent, and the microcystin fractions of both N-treatments are similar for most of the microcystin variants. In the N-replete treatments, the microcystin fractions remained mostly unchanged with increasing $p\text{CO}_2(\text{aq})$ except for MC-LR (NIES 1099 and HUB 524) and MC-LW (PCC 7820).

3.4. Relating microcystins to N:C stoichiometry

How do the microcystin content and composition of the cells vary with cellular N:C ratios as well as absolute cellular N and C contents? At low $p\text{CO}_2(\text{aq})$, the cellular N:C ratios clustered at intermediate N- and C-contents with a mean N:C ratio of 0.13 for both N-treatments (Fig. 5. A). With increasing $p\text{CO}_2(\text{aq})$ in the N-replete treatment, the N-content increased and/or the C-content decreased, causing the observed shift toward high N:C ratios reaching values up to 0.16. Conversely, under N-

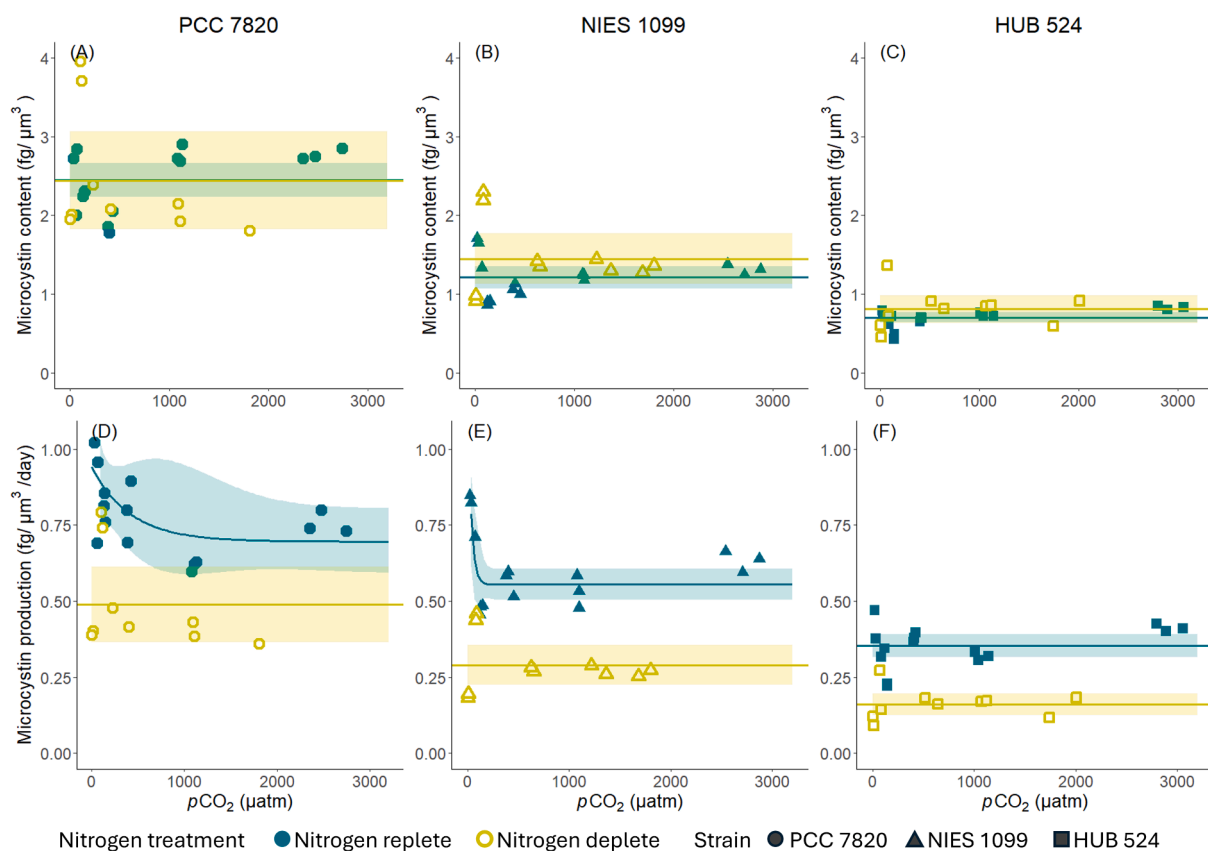


Fig. 3. Cellular microcystin content (A–C) and microcystin production rate (D–F) in the N-replete and N-deplete treatments across the $p\text{CO}_2(\text{aq})$ gradient for *Microcystis aeruginosa* strain PCC 7820 (A, D), NIES 1099 (B, E), HUB 524 (C, F). Lines show the fit of an asymptotic model if two or more of the model parameters were significant ($p < 0.05$); otherwise, the lines show the mean of all points for the N-replete and N-deplete treatments. The shaded ribbons indicate the 95 % confidence interval of the model.

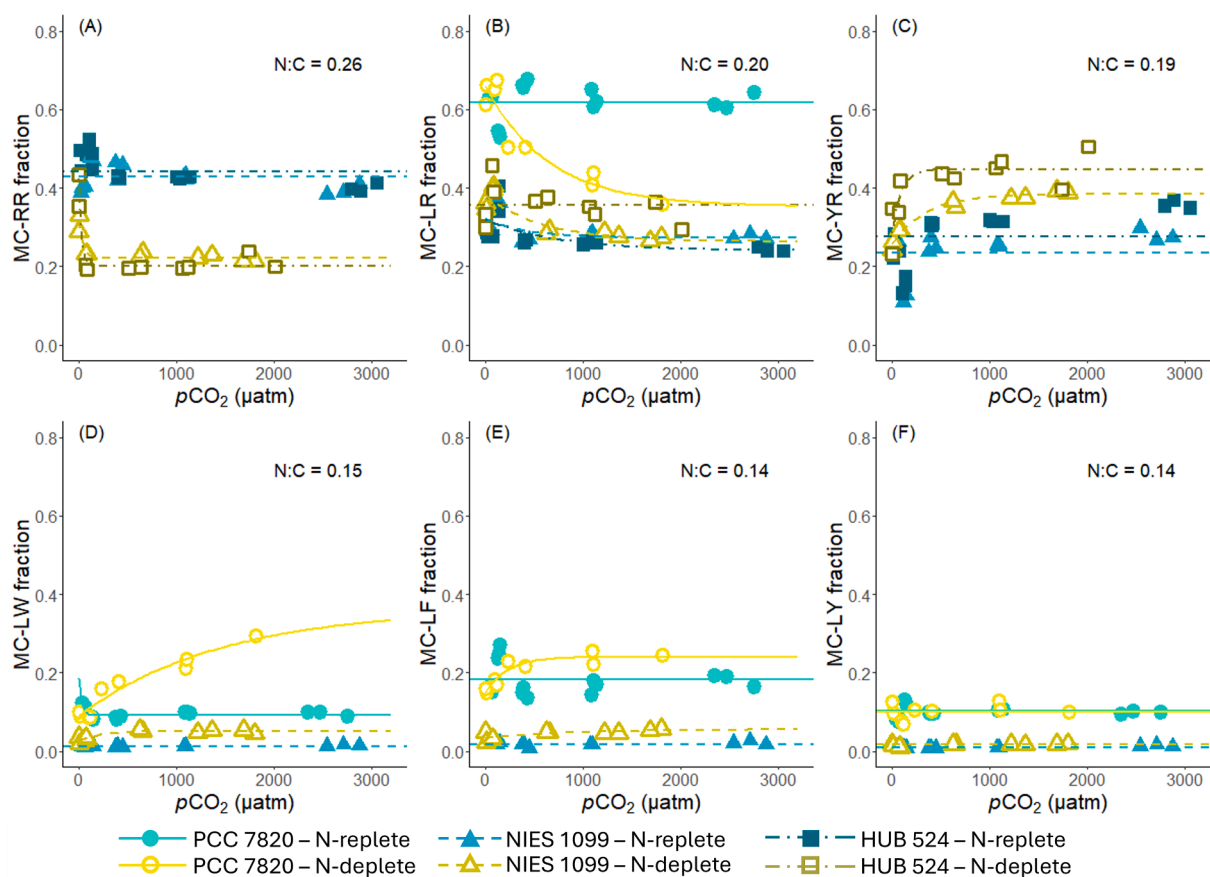


Fig. 4. Relative contribution of the microcystin variants MC-RR (A), MC-LR (B), MC-YR (C), MC-LW (D), MC-LF (E), and MC-LY (F) to the total microcystin content, for the three strains of *Microcystis aeruginosa* in the N-replete and N-deplete treatments across the $p\text{CO}_2(\text{aq})$ gradient. All microcystin variants were found in at least two of the strains and MC-LR was found in all three strains. Lines show the fit of an asymptotic model if two or more of the model parameters were significant ($p < 0.05$); otherwise, the lines show the mean of all points for the N-replete and N-deplete treatments.

deplete conditions, the N-content decreased, and the C-content remained the same or decreased slightly, causing a decrease in cellular N:C ratios down to 0.07. We did not observe a consistent trend in microcystin content across the changes in N- and C- contents (Fig. 5. B). Yet, the results show distinct stoichiometric relationships in microcystin composition, which were particularly clear for MC-RR, -YR, -LW and -LF (Fig. 5. C-D, S4B-C). For example, the fraction of the N-rich microcystin variant MC-RR is lowest at low cellular N:C ratios, while MC-YR, LW and LF are highest at low cellular N:C ratios (Fig. 5. C,D, S4B-C).

4. Discussion

Our results showed consistent and interactive effects of increasing $p\text{CO}_2(\text{aq})$ and nitrogen availability on the cellular N:C stoichiometry for all three strains. The results are partly in line with our first hypothesis, as N:C ratios indeed decreased with increasing $p\text{CO}_2(\text{aq})$ in the N-deplete treatments. Contrary to expectation, however, increasing $p\text{CO}_2(\text{aq})$ caused an increase in N:C ratios in the N-replete treatments. The changes in N:C stoichiometry were mainly driven by shifts in the cellular nitrogen contents, that decreased with increasing $p\text{CO}_2(\text{aq})$ in the N-deplete treatments but generally increased in the N-replete treatments (for NIES 1099 and HUB 524). In contrast to our second hypothesis, increasing $p\text{CO}_2(\text{aq})$ did not lead to significant changes in microcystin content. However, microcystin production rates decreased with increasing $p\text{CO}_2(\text{aq})$ in the N-replete treatments of PCC 7820 and NIES 1099, and were generally lower under N-deplete than under N-replete conditions, following the lower N:C ratios under N-deplete conditions. The changes in microcystin composition were largely in line with our third

hypothesis and followed changes in N:C ratios. That is, MC-RR was more prevalent at high cellular N:C ratios under N-replete conditions, whereas MC-YR, MC-LW and MC-LF were more prevalent at low cellular N:C ratios under N-deplete conditions.

4.1. Growth and carbon acquisition

Impacts of changes in $p\text{CO}_2(\text{aq})$ on *Microcystis* strains will depend on their carbon acquisition strategies, which may be reflected in the growth responses (Sandrini et al., 2014). While growth rates were fixed by the dilution rates in our N-deplete treatments, the growth rates decreased with increasing $p\text{CO}_2(\text{aq})$ under N-replete conditions (Fig. S2). This decrease was more apparent for PCC 7820 than for NIES 1099 and HUB 524 (Table S4, A and B parameters). Apparently, high $p\text{CO}_2(\text{aq})$ constrains growth of these three *Microcystis* strains under N-replete conditions. One possible explanation is that the tested strains have carbon concentrating mechanisms (CCMs) that perform well at low $p\text{CO}_2(\text{aq})$ but not at high $p\text{CO}_2(\text{aq})$. Cyanobacteria have five inorganic carbon (Ci) uptake systems that facilitate inorganic carbon acquisition at a wide range of CO_2 and bicarbonate levels. Three of these uptake systems (NDH-I₃, NDH-I₄, BCT1) have been found in all 20 strains of *Microcystis aeruginosa* investigated thus far, while the presence of the other two uptake systems (*bicA* and *sbtA*) differs among strains (Sandrini et al., 2014). Both these systems are bicarbonate uptake systems, with *sbtA* having high affinity for bicarbonate but low flux rate, and *bicA* having low affinity but high flux rate. With increasing $p\text{CO}_2(\text{aq})$, pH in our experiments decreased and dissolved inorganic carbon (DIC) speciation moved towards higher concentrations of dissolved CO_2 . Furthermore,

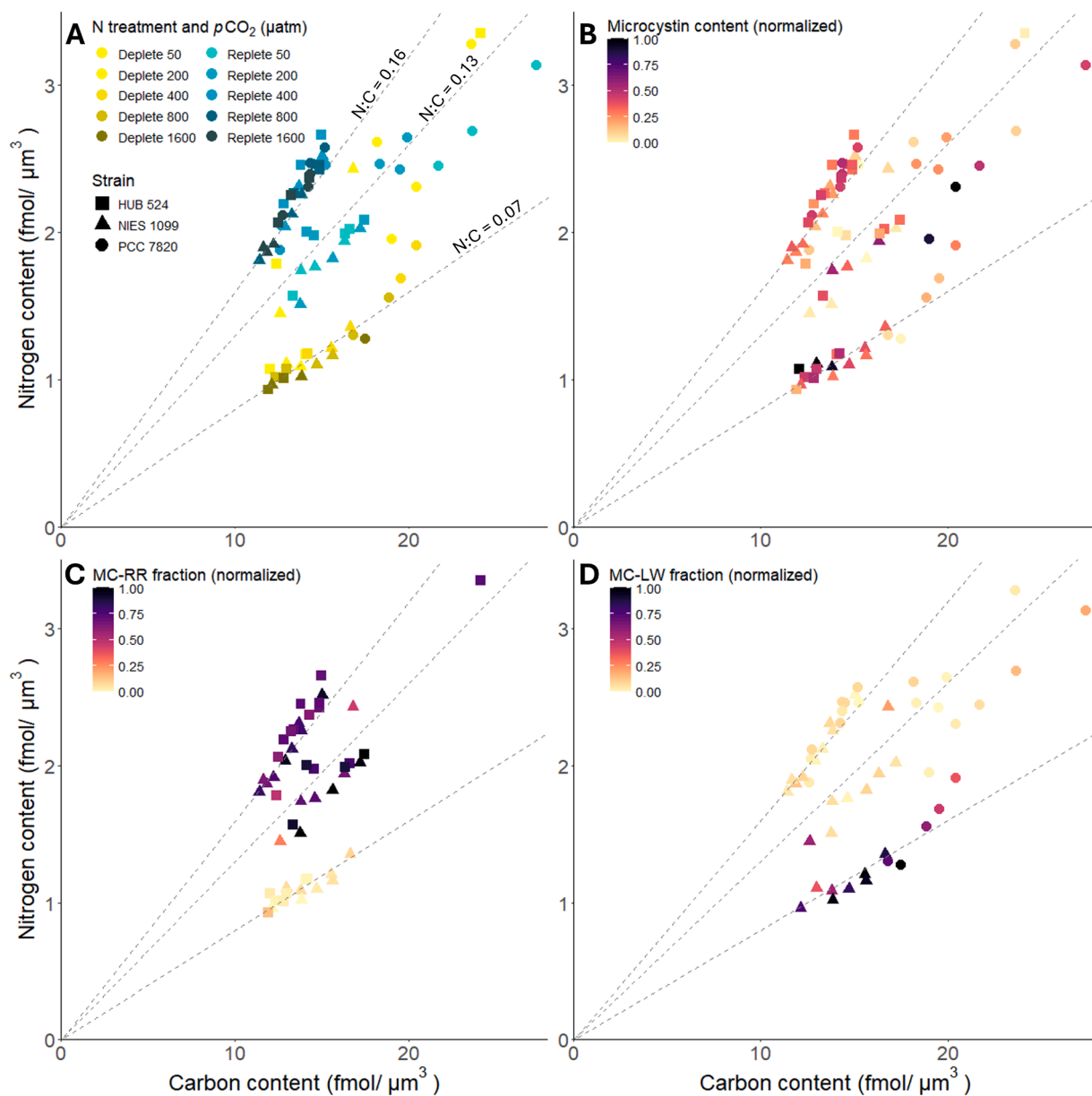


Fig. 5. Cellular nitrogen and carbon contents of the three strains of *Microcystis aeruginosa* in the N-replete (blue symbols) and N-deplete (yellow symbols) treatments (A). The microcystin content (B) and fractions of MC-RR (C) and MC-LW (D) as a function of the cellular nitrogen and carbon content for the three strains of *Microcystis aeruginosa*. The dotted lines represent molar N:C ratios of 0.16, 0.13 and 0.07. Microcystin content (B) and composition of MC-RR (C) and MC-LR (D) were normalized to the maximum value measured within the respective strain.

although the relative amount of HCO_3^- as fraction of the total DIC declined, the absolute concentration of HCO_3^- increased with increasing $p\text{CO}_2(\text{aq})$, in line with previous studies (Verspagen et al. 2014a). At elevated $p\text{CO}_2(\text{aq})$, strains with the *bicA* gene were shown to increase their specific growth rate, while strains with the *sbtA* gene decreased theirs (Sandrini et al., 2014; Zheng et al., 2023). The HUB 524 strain used in our study only has the high affinity low flux rate *sbtA* gene, which is consistent with the observed decrease in growth rate with increasing $p\text{CO}_2(\text{aq})$. The Ci uptake genes of the PCC 7820 and NIES 1099 strains have not been analyzed but their decreased growth rates in high $p\text{CO}_2(\text{aq})$ environments suggest that they potentially belong to the *sbtA* genotype as well, similar to HUB 524. Differences in Ci uptake mechanisms across different genotypes may lead to a succession of dominant genotypes of *Microcystis* throughout a bloom (Sandrini et al., 2016; Jiang et al., 2024). Moreover, changes in $p\text{CO}_2(\text{aq})$ can change the resource that is limiting, for example from CO_2 to light (Kardinaal et al.,

2007b; Van de Waal et al., 2011) or nitrogen (Wang et al., 2019), and thereby affect the intraspecific competition between genotypes.

4.2. N:C stoichiometry

The changes in cellular N:C ratios were highly consistent across the three strains. We hypothesized that in both N-treatments, cellular N:C stoichiometry will decrease with increasing $p\text{CO}_2(\text{aq})$, however, to a greater extent in the N-deplete treatments. Our results showed that indeed, in the N-deplete treatments, the increase in $p\text{CO}_2(\text{aq})$ led to a decrease in N:C ratios. However, in the N-replete treatment, an increase in $p\text{CO}_2(\text{aq})$ led to an increase in N:C stoichiometry, partially refuting our hypothesis. At the same time, an increase in $p\text{CO}_2(\text{aq})$ did increase the difference between the N:C ratios of the N-deplete versus N-replete treatment, as was expected. We thus observed a distinct interactive effect, where N:C ratios in response to differences in nitrogen availability

were modulated by changes in $p\text{CO}_2(\text{aq})$. Under low $p\text{CO}_2(\text{aq})$ ($<100 \mu\text{atm}$) the cells exhibited intermediate N:C ratios, while at higher $p\text{CO}_2(\text{aq})$ ($> 100 \mu\text{atm}$), the N:C ratios either decreased or increased (Fig. 2). These changes confirm the different physiological conditions, with nitrogen limitation or non-limited growth at higher $p\text{CO}_2(\text{aq})$, and carbon limitation and/or a co-limitation of carbon and nitrogen (for the N-deplete treatments) at low $p\text{CO}_2(\text{aq})$. The differences in N:C ratios between the nitrogen treatments follow earlier reported stoichiometric responses of phytoplankton to N-limitation (Tanioka and Matsumoto, 2020). Only a limited number of studies have reported phytoplankton stoichiometric responses to carbon limitation, which varied from intermediate N:C ratios comparable to our study (Van de Waal et al., 2009) to relatively high N:C ratios (Verspagen et al., 2014b). Our findings suggest that nitrogen assimilation may be hampered by carbon limitation, which follows from the close coupling between nitrogen and carbon metabolism (Flores and Herrero, 2005; Zhang et al., 2018).

Cellular N:C ratios vary because of changes in the cellular N- and/or C-contents. The observed shifts in the cellular contents of nitrogen and carbon were different for PCC 7820 compared to the other two strains. For PCC 7820, both the N- and C-contents decreased with increasing $p\text{CO}_2(\text{aq})$ under N-replete conditions (Figs. 1, 5A). This decrease was stronger for carbon than nitrogen, leading to an increase in N:C ratios. As for NIES 1099 and HUB 524, the N-content increased with increasing $p\text{CO}_2(\text{aq})$ in the N-replete treatments, while C-content decreased slightly. These findings suggest that elevated $p\text{CO}_2(\text{aq})$ can facilitate enhanced nitrogen acquisition, at least for two of the strains in our study (i.e., NIES 1099 and HUB 524). This can be explained through the assimilation pathways of nitrogen in cyanobacteria. Inorganic nitrogen is converted to ammonium before assimilation into organic molecules. Following the conversion to ammonium, there are two assimilation pathways: 1) the glutamine synthetase-glutamate synthase (GS-GOGAT) cycle, and 2) direct assimilation through glutamate dehydrogenase (GDH). Both assimilation pathways in cyanobacteria require the carbon skeleton 2-oxoglutarate (2-OG), which is an intermediate product in the citric acid cycle. Therefore, 2-OG provides the basis for the tight coupling between carbon and nitrogen metabolism. In other words, in the presence of excess nitrogen, an increase in CO_2 will promote the synthesis of 2-OG and thereby enhance nitrogen assimilation (Zhang et al., 2018). In contrast, a lower nitrogen availability will constrain the assimilation of nitrogen-rich biochemicals such as proteins (Allen, 1984; Gobler et al., 2016), which can explain the lower cellular nitrogen contents and N:C ratios observed across the three strains under N-deplete conditions (Fig. 1. D–F). Overall, our results show that the responses of the cellular N-contents and C-contents to increasing $p\text{CO}_2$ varied among the *Microcystis* strains (i.e., PCC 7820 showed a deviating response), whereas changes in cellular N:C stoichiometry were consistent among the strains.

4.3. Stoichiometry, growth and microcystin synthesis

In contrast to our second hypothesis, the total microcystin content did not follow responses in N:C ratios and remained unaffected by increasing $p\text{CO}_2(\text{aq})$ and nitrogen availability. We expected a reduced microcystin content under low N:C ratios, particularly in response to nitrogen limitation (Van de Waal et al., 2014; Wagner et al., 2019; Brandenburg et al., 2020). When assessing microcystin quota (i.e. the amount of microcystin per cell, rather than biovolume), we observed lower levels in both PCC 7820 and NIES 1099 under N-deplete treatments (Fig. S3). These findings illustrate that decreases in cellular microcystin levels can be proportional or stronger compared to shifts in cell size and indicate the importance of considering cell size when reporting relationships between microcystin synthesis and environmental conditions.

Nitrogen availability may impact microcystin synthesis indirectly by causing shifts in growth rates. Earlier work showed that faster growing cells that were less limited in nitrogen produced more microcystin than

slower growing cells that were more strongly limited in nitrogen (Long et al., 2001). In other words, growth rate and the extent of nitrogen limitation are closely associated, and reduced microcystin production may be caused by reduced growth directly as well as by a decrease in available nitrogen to produce microcystin (Gobler et al., 2016). Indeed, when correcting for growth rates, we observed consistently lower microcystin production rates (Fig. 3. D–F) under N-deplete than under N-replete conditions. Thus, nitrogen seems to play a key role in regulating microcystin production directly by shifting N-assimilation, and/or indirectly through changes in growth rates.

4.4. Microcystin composition

The composition of microcystin showed strong responses to nitrogen availability, which partly reflected the changes in cellular N:C ratios (Figs. 4, 5, Fig. S4). Similar to N:C ratios, shifts in microcystin composition were consistent across strains, which points to a major impact of N:C stoichiometry on the composition of microcystin variants. The effect of $p\text{CO}_2(\text{aq})$ was particularly apparent in the N-deplete treatments, while the microcystin composition remained largely unaffected by increasing $p\text{CO}_2(\text{aq})$ under N-replete conditions. When nitrogen was limiting, an increase in $p\text{CO}_2(\text{aq})$ caused a decrease in cellular N:C ratios, which favored the less N-containing variants MC-YR, -LW and -LF over the N-richer variants MC-RR and -LR. This is in line with previous studies and confirms that the synthesis of different microcystin variants within the cell is closely connected to carbon and nitrogen metabolism (Van de Waal et al., 2009; Ginn et al., 2010; Alexova et al., 2011; Kuniyoshi et al., 2011; Wei et al., 2024). Specifically, we observed strong changes in the fraction of the N-richest microcystin variant MC-RR that was favored under N-replete conditions and decreased under N-deplete conditions with increasing $p\text{CO}_2(\text{aq})$ (Fig. 4. A). The least N-containing microcystin variants MC-LY (in NIES 1099), MC-LW (in PCC 7820 and NIES 1099) and MC-LF (in PCC 7820 and NIES 1099) showed the opposite response (Fig. 4. D–F, Table S5). This confirms our third hypothesis and is in line with earlier observations in laboratory experiments (Van de Waal et al., 2009; Liu et al., 2016), and in the field (Van de Waal et al., 2009; Chaffin et al., 2023). The shifts in microcystin composition may reflect underlying changes in the metabolism of amino acids that are required for the different microcystin variants. For example, MC-LW contains tryptophan (W) which is an amino acid whose pathway is closely related to carbon metabolism. The carbon skeleton of aromatic amino acids like tryptophan (W), phenylalanine (F), and tyrosine (Y) are derived from two intermediate products from glycolysis and the pentose phosphate pathway (PPP) or Calvin Cycle (CC), all closely related to carbon metabolism (Ainsworth et al., 2006; Li et al., 2008). Accordingly, we expect higher CO_2 and/or low nitrogen availability to specifically promote the synthesis of MC-LW, -LF and -LY, as under these conditions the carbon metabolism is relatively stimulated. This was indeed observed where MC-YR, MC-LW and MC-LF, and partly MC-LY, were higher under N-deplete conditions, while MC-YR, MC-LW, and MC-LF were also higher at high $p\text{CO}_2(\text{aq})$ as compared to low $p\text{CO}_2(\text{aq})$ conditions. On the other hand, MC-RR contains two arginine, which is synthesized from glutamate (Glu) and glutamine (Gln) that are products of nitrogen assimilation through the glutamine synthetase–glutamate synthase pathways. Hence, N-limitation is expected to affect the synthesis of arginine the most, and consequently the N-rich variant MC-RR. This was confirmed by our results, showing consistently lower MC-RR contents in the N-deplete than in the N-replete treatments. For MC-LR we observed differential responses to N-limitation between the strains, where the N-deplete conditions showed a lower MC-LR content in PCC 7820, no change in NIES 1099, and a higher MC-LR content in HUB 524 compared to the N-replete conditions at high $p\text{CO}_2(\text{aq})$.

4.5. Implications for bloom toxicity

Our results show that changes in cellular N:C stoichiometry in

response to elevated $p\text{CO}_2(\text{aq})$ and N-limitation were very similar for all three strains (Fig. 2). As discussed above, interactions between nitrogen and carbon metabolism play a major role in amino acid synthesis. Therefore, changes in N:C stoichiometry of the cells can alter the variable amino acids in microcystin molecules, and hence the microcystin variant composition. In line with expectation and with earlier findings (Van de Waal et al., 2009; Chaffin et al., 2023), the composition of N-rich microcystin variants (e.g., MC-RR) was higher at high cellular N:C ratios, whereas the composition of less N-containing microcystin variants (e.g., MC-LW and MC-LF) was higher at low N:C ratios. These microcystin variants differ in toxicity (Table 1). Hence, our results indicate that, within the set of variants they are capable of producing, microcystin-producing cyanobacteria are likely to shift production to relatively N-rich microcystin variants of lower toxicity in lakes when nitrogen is available in excess, whereas under N-limited conditions they are more likely to favor less N-containing microcystin variants of high toxicity. Moreover, our results show that the cellular N:C stoichiometry decreased with increasing $p\text{CO}_2(\text{aq})$ under N-deplete conditions, but contrary to expectation it increased with increasing $p\text{CO}_2(\text{aq})$ under N-replete conditions. Hence, differences in N:C stoichiometry and microcystin variant composition became pronounced at elevated $p\text{CO}_2$. Translation of these laboratory results to cyanobacterial blooms in lakes would imply that, at elevated $p\text{CO}_2$, cyanobacteria in lakes with high nitrogen availability will produce relatively more N-rich microcystin variants of lower toxicity, whereas under N-limited conditions, they will produce relatively more microcystin variants containing less nitrogen but with higher toxicity.

All three strains showed qualitatively similar patterns in microcystin compositional changes. Hence, our findings indicate that changes in CO_2 and nitrogen availability will alter the microcystin variant composition of cyanobacterial genotypes in a stoichiometrically predictable way. However, genotypes differ in the innate set of microcystin variants they are capable of producing, as well as in their growth rates and total microcystin content. In the field, this translates to observing shifts in microcystin composition and total microcystin concentration as genotypic composition changes throughout a bloom (Kardinaal et al., 2007a; Chaffin et al., 2023). Hence, how the microcystin composition and total microcystin concentration in lakes will be affected by changes in CO_2 and nitrogen availability will strongly depend on the wax and wane of different genotypes.

CRedit authorship contribution statement

Savannah Sarkis: Writing – review & editing, Writing – original draft, Visualization, Validation, Software, Resources, Project administration, Methodology, Investigation, Formal analysis, Data curation, Conceptualization. **Jing Liu:** Writing – review & editing, Methodology, Investigation, Formal analysis, Data curation, Conceptualization. **Jef Huisman:** Writing – review & editing, Visualization, Validation, Supervision, Resources, Methodology, Investigation, Formal analysis, Data curation, Conceptualization. **Uwe John:** Writing – review & editing, Supervision, Formal analysis, Conceptualization. **Jolanda M.H. Ver-spagen:** Writing – review & editing, Validation, Methodology, Investigation, Data curation. **Dedmer B. Van de Waal:** Writing – review & editing, Visualization, Validation, Supervision, Resources, Project administration, Methodology, Investigation, Funding acquisition, Formal analysis, Data curation, Conceptualization.

Declaration of competing interest

The authors declare that they have no known competing financial interests or personal relationships that could have appeared to influence the work reported in this paper.

Acknowledgements

The authors thank Nico Helmsing for nutrient analysis, Erik Reichman for microcystin measurements, and Yoeri Kraak for help with the experiment. SS and DBVW were funded by the European Union (ERC, BLOOMTOX, project number 101044452). Views and opinions expressed are however those of the author(s) only and do not necessarily reflect those of the European Union or the European Research Council Executive Agency. Neither the European Union nor the granting authority can be held responsible for them. UJ was funded by the Helmholtz research program “Changing Earth, Sustaining our Future” (Subtopic 6.2 Adaptation of marine life) of the Alfred Wegener Institute Helmholtz Centre for Polar and Marine Research.

Supplementary materials

Supplementary material associated with this article can be found, in the online version, at [doi:10.1016/j.hal.2025.102964](https://doi.org/10.1016/j.hal.2025.102964).

Data availability

The data used in this study are available in the open data repository DataverseNL at <https://doi.org/10.34894/W5IA98>.

References

- Ainsworth, E.A., Rogers, A., Vodkin, L.O., Walter, A., Schurr, U., 2006. The effects of elevated CO_2 concentration on soybean gene expression. An analysis of growing and mature leaves. *Plant Physiol.* 142, 135–147. <https://doi.org/10.1104/pp.106.086256>.
- Alexova, R., Haynes, P.A., Ferrari, B.C., Neilan, B.A., 2011. Comparative protein expression in different strains of the bloom-forming cyanobacterium *Microcystis aeruginosa*. *Mol. Cell. Proteomics* 10, M110.003749. <https://doi.org/10.1074/mcp.M110.003749>.
- Allen, M.M., 1984. Cyanobacterial cell inclusions. *Annu. Rev. Microbiol.* 38, 1–25. <https://doi.org/10.1146/annurev.mi.38.100184.000245>.
- Balmer, M., Downing, J., 2011. Carbon dioxide concentrations in eutrophic lakes: undersaturation implies atmospheric uptake. *Inland Waters* 1, 125–132. <https://doi.org/10.5268/iw-1.2.366>.
- Bouaïcha, N., Miles, C.O., Beach, D.G., Labidi, Z., Djabri, A., Benayache, N.Y., Nguyen-Quang, T., 2019. Structural diversity, characterization and toxicology of microcystins. *Toxins* 11, 714. <https://doi.org/10.3390/toxins11120714>.
- Brandenburg, K., Siebers, L., Keuskamp, J., Jephcott, T.G., Van de Waal, D.B., 2020. Effects of nutrient limitation on the synthesis of N-rich phytoplankton toxins: a meta-analysis. *Toxins* 12, 221. <https://doi.org/10.3390/toxins12040221>.
- Carmichael, W.W., 2001. Health effects of toxin-producing cyanobacteria: “The Cyanobacteria”. *Hum. Ecol. Risk Assess.* 7, 1393–1407. <https://doi.org/10.1080/20018091095087>.
- Chaffin, J.D., Westrick, J.A., Reitz, L.A., Bridgeman, T.B., 2023. Microcystin congeners in Lake Erie follow the seasonal pattern of nitrogen availability. *Harmful Algae* 127, 102466. <https://doi.org/10.1016/j.hal.2023.102466>.
- Chorus, I., Welker, M., 2021. *Toxic Cyanobacteria in Water*, 2nd ed. CRC Press.
- Cole, J.J., Caraco, N.F., Kling, G.W., Kratz, T.K., 1994. Carbon dioxide supersaturation in the surface waters of lakes. *Science* 265, 5178. <https://doi.org/10.1126/science.265.5178.1568>.
- Downing, T.G., Meyer, C., Gehring, M.M., Van De Venter, M., 2005. Microcystin content of *Microcystis aeruginosa* is modulated by nitrogen uptake rate relative to specific growth rate or carbon fixation rate. *Environ. Toxicol.* 20, 257–262. <https://doi.org/10.1002/tox.20106>.
- Flores, E., Herrero, A., 2005. Nitrogen assimilation and nitrogen control in cyanobacteria. *Biochem. Soc. Trans.* 33, 164–167.
- Faassen, E.J., Lürling, M., 2013. Occurrence of the microcystins MC-LW and MC-LF in Dutch surface waters and their contribution to total microcystin toxicity. *Mar. Drugs* 11, 2643–2654. <https://doi.org/10.3390/md11072643>.
- Fischer, A., Hoeger, S.J., Stemmer, K., Feurstein, D.J., Knobloch, D., Nussler, A., Dietrich, D.R., 2010. The role of organic anion transporting polypeptides (OATPs/SLCOs) in the toxicity of different microcystin congeners *in vitro*: a comparison of primary human hepatocytes and OATP-transfected HEK293 cells. *Toxicol. Appl. Pharmacol.* 245, 9–20. <https://doi.org/10.1016/j.taap.2010.02.006>.
- Ginn, H.P., Pearson, L.A., Neilan, B.A., 2010. NtcA from *Microcystis aeruginosa* PCC 7806 is autoregulatory and binds to the microcystin promoter. *Appl. Environ. Microbiol.* 76, 4362–4368. <https://doi.org/10.1128/AEM.01862-09>.
- Gobler, C.J., Burkholder, J.A.M., Davis, T.W., Harke, M.J., Johengen, T., Stow, C.A., Van de Waal, D.B., 2016. The dual role of nitrogen supply in controlling the growth and toxicity of cyanobacterial blooms. *Harmful Algae* 54, 87–97. <https://doi.org/10.1016/j.hal.2016.01.010>.
- Harke, M.J., Gobler, C.J., 2015. Daily transcriptome changes reveal the role of nitrogen in controlling microcystin synthesis and nutrient transport in the toxic

- cyanobacterium, *Microcystis aeruginosa*. BMC Genomics 16, 1. <https://doi.org/10.1186/s12864-015-2275-9>.
- Harper, D., 1992. Eutrophication of freshwaters: principles, problems and restoration. <https://api.semanticscholar.org/CorpusID:129067801>.
- Huisman, J., Codd, G.A., Paerl, H.W., Ibelings, B.W., Verspagen, J.M.H., Visser, P.M., 2018. Cyanobacterial blooms. Nat. Rev. Microbiol. 16, 471–483. <https://doi.org/10.1038/s41579-018-0040-1>.
- Huisman, J., Matthijs, H.C.P., Visser, P.M., Balke, H., Sigon, C.A.M., Passarge, J., Weissing, F.J., Mur, L.R., 2002. Principles of the light-limited chemostat: theory and ecological applications. Antonie van Leeuwenhoek 81, 117–133. <https://doi.org/10.1023/A:1020537928216>.
- Ji, X., Verspagen, J.M., Van de Waal, D.B., Rost, B., Huisman, J., 2020. Phenotypic plasticity of carbon fixation stimulates cyanobacterial blooms at elevated CO₂. Sci. Adv. 6, eaax2926. <https://doi.org/10.1126/sciadv.aax2926>.
- Jiang, J., Zeng, J., Wang, J., Zuo, J., Wei, N., Song, L., Shan, K., Gan, N., 2024. Changes in CO₂ concentration drive a succession of toxic and non-toxic strains of *Microcystis* blooms. Water Res. 250, 121056. <https://doi.org/10.1016/j.watres.2023.121056>.
- Johansson, E., Legrand, C., Björnerås, C., Godhe, A., Mazur-Marzec, H., Säll, T., Rengefors, K., 2019. High diversity of microcystin chemotypes within a summer bloom of the cyanobacterium *Microcystis botrys*. Toxins 11, 698. <https://doi.org/10.3390/toxins11120698>.
- Kardinaal, E., Janse, I., Kamst-van Agterveld, M., Meima, M., Snoek, J., Mur, L.R., Huisman, J., Zwart, G., Visser, P.M., 2007a. *Microcystis* genotype succession in relation to microcystin concentrations in freshwater lakes. Aquat. Microb. Ecol. 48, 1–12. <https://doi.org/10.3354/ame048001>.
- Kardinaal, E., Tonk, L., Janse, I., Hol, S., Slot, P., Huisman, J., Visser, P.M., 2007b. Competition for light between toxic and nontoxic strains of the harmful cyanobacterium *Microcystis*. Appl. Environ. Microbiol. 73, 2939–2946. <https://doi.org/10.1128/AEM.02892-06>.
- Kilham, S.S., Kreeger, D.A., Lynn, S.G., Goulden, C.E., Herrera, L., 1998. COMBO: a defined freshwater culture medium for algae and zooplankton. Hydrobiologia 377, 147–159. <https://doi.org/10.1023/A:1003231628456>.
- Kuniyoshi, T.M., Gonzalez, A., Lopez-Gomollon, S., Valladares, A., Bes, M.T., Fillat, M.F., Peleato, M.L., 2011. 2-oxoglutarate enhances NtcA binding activity to promoter regions of the microcystin synthesis gene cluster. FEBS Lett. 585, 3921–3926. <https://doi.org/10.1016/j.febslet.2011.10.034>.
- Lazzarino, J.K., Bachmann, R.W., Hoyer, M.V., Canfield, D.E., 2009. Carbon dioxide supersaturation in Florida lakes. Hydrobiologia 627, 169–180. <https://doi.org/10.1007/s10750-009-9723-y>.
- Li, P., Ainsworth, E.A., Leakey, A.D.B., Ulanov, A., Lozovaya, V., Ort, D.R., Bohnert, H.J., 2008. Arabidopsis transcript and metabolite profiles: ecotype-specific responses to open-air elevated [CO₂]. Plant Cell Environ. 31, 1673–1687. <https://doi.org/10.1111/j.1365-3040.2008.01874.x>.
- Liu, J., van Oosterhout, E., Faassen, E.J., Lürling, M., Helmsing, N.R., Van de Waal, D.B., 2016. Elevated pCO₂ causes a shift towards more toxic microcystin variants in nitrogen limited *Microcystis aeruginosa*. FEMS Microbiol. Ecol. 92, fiv159. <https://doi.org/10.1093/femsec/fiv159>.
- Long, B.M., Jones, G.J., Orr, P.T., 2001. Cellular microcystin content in N-limited *Microcystis aeruginosa* can be predicted from growth rate. Appl. Environ. Microbiol. 67, 278–283. <https://doi.org/10.1128/AEM.67.1.278-283.2001>.
- Maberly, S.C., 1996. Diel, episodic and seasonal changes in pH and concentrations of inorganic carbon in a productive lake. Freshwater Biol. 35, 579–598. <https://doi.org/10.1111/j.1365-2427.1996.tb01770.x>.
- Meissner, S., Fastner, J., Dittmann, E., 2013. Microcystin production revisited: conjugate formation makes a major contribution. Environ. Microbiol. 15, 1810–1820. <https://doi.org/10.1111/1462-2920.12072>.
- Meriluoto, J., Spoof, L., Codd, G.A., 2017. Handbook of Cyanobacterial Monitoring and Cyanotoxin Analysis. John Wiley & Sons. <https://doi.org/10.1002/9781119068761>.
- O’Neil, J.M., Davis, T.W., Burford, M.A., Gobler, C.J., 2012. The rise of harmful cyanobacteria blooms: the potential roles of eutrophication and climate change. Harmful Algae 14, 313–334. <https://doi.org/10.1016/j.hal.2011.10.027>.
- Paerl, H.W., Huisman, J., 2008. Blooms like it hot. Science 320, 57–58. <https://doi.org/10.1126/science.1155398>.
- Price, D., Woodger, F.J., Badger, M.R., Howitt, S.M., Tucker, L., 2004. Identification of a SulP-type bicarbonate transporter in marine cyanobacteria. Proc. Natl. Acad. Sci. USA 101 (52), 18228–18233. <https://doi.org/10.1073/pnas.0405211101>.
- Sandrini, G., Ji, X., Verspagen, J.M.H., Tann, R.P., Slot, P.C., Luimstra, V.M., Schuurmans, J.M., Matthijs, H.C.P., Huisman, J., 2016. Rapid adaptation of harmful cyanobacteria to rising CO₂. Proc. Natl. Acad. Sci. USA 113 (33), 9315–9320. <https://doi.org/10.1073/pnas.1602435113>.
- Sandrini, G., Matthijs, H.C.P., Verspagen, J.M.H., Muyzer, G., Huisman, J., 2014. Genetic diversity of inorganic carbon uptake systems causes variation in CO₂ response of the cyanobacterium *Microcystis*. ISME J. 8 (3), 589–600. <https://doi.org/10.1038/ismej.2013.179>.
- Talling, J.F., 1976. The depletion of carbon dioxide from lake water. J. Ecol. 64 (1), 79–121.
- Tanioka, T., Matsumoto, K., 2020. A meta-analysis on environmental drivers of marine phytoplankton C: N: P. Biogeosciences 17 (11), 2939–2954. <https://doi.org/10.5194/bg-17-2939-2020>.
- Van de Waal, D.B., Ferreruela, G., Tonk, L., Van Donk, E., Huisman, J., Visser, P.M., Matthijs, H.C.P., 2010. Pulsed nitrogen supply induces dynamic changes in the amino acid composition and microcystin production of the harmful cyanobacterium *Planktothrix agardhii*. FEMS Microbiol. Ecol. 74 (2), 430–438. <https://doi.org/10.1111/j.1574-6941.2010.00958.x>.
- Van de Waal, D.B., Smith, V.H., Declerck, S.A.J., Stam, E.C.M., Elser, J.J., 2014. Stoichiometric regulation of phytoplankton toxins. Ecol. Lett. 17 (6), 736–742. <https://doi.org/10.1111/ele.12280>.
- Van de Waal, D.B., Verspagen, J.M.H., Finke, J.F., Vournazou, V., Immers, A.K., Kardinaal, W.E.A., Tonk, L., Becker, S., Van Donk, E., Visser, P.M., Huisman, J., 2011. Reversal in competitive dominance of a toxic versus non-toxic cyanobacterium in response to rising CO₂. ISME J. 5 (9), 1438–1450. <https://doi.org/10.1038/ismej.2011.28>.
- Van de Waal, D.B., Verspagen, J.M.H., Lürling, M., Van Donk, E., Visser, P.M., Huisman, J., 2009. The ecological stoichiometry of toxins produced by harmful cyanobacteria: an experimental test of the carbon-nutrient balance hypothesis. Ecol. Lett. 12 (12), 1326–1335. <https://doi.org/10.1111/j.1461-0248.2009.01383.x>.
- Verspagen, J.M.H., Van de Waal, D.B., Finke, J.F., Visser, P.M., Van Donk, E., Huisman, J., 2014a. Rising CO₂ levels will intensify phytoplankton blooms in eutrophic and hypertrophic lakes. PLoS ONE 9 (8), 104325. <https://doi.org/10.1371/journal.pone.0104325>.
- Verspagen, J.M.H., Van de Waal, D.B., Finke, J.F., Visser, P.M., Huisman, J., 2014b. Contrasting effects of rising CO₂ on primary production and ecological stoichiometry at different nutrient levels. Ecol. Lett. 17 (8), 951–960. <https://doi.org/10.1111/ele.12298>.
- Vézic, C., Rapala, J., Vaitoama, J., Seitonen, J., Sivonen, K., 2002. Effect of nitrogen and phosphorus on growth of toxic and nontoxic *Microcystis* strains and on intracellular microcystin concentrations. Microb. Ecol. 43 (4), 443–454. <https://doi.org/10.1007/s00248-001-0041-9>.
- Wagner, N.D., Osburn, F.S., Wang, J., Taylor, R.B., Boedecker, A.R., Chambliss, C.K., Brooks, B.W., Scott, J.T., 2019. Biological stoichiometry regulates toxin production in *Microcystis aeruginosa* (UTEX 2385). Toxins 11 (10), 601. <https://doi.org/10.3390/toxins11100601>.
- Wang, Z., Zhang, Y., Huang, S., Peng, C., Hao, Z., Li, D., 2019. Nitrogen limitation significantly reduces the competitive advantage of toxic *Microcystis* at high light conditions. Chemosphere 237, 124508. <https://doi.org/10.1016/j.chemosphere.2019.124508>.
- Wei, N., Hu, C., Dittmann, E., Song, L., Gan, N., 2024. The biological functions of microcystins. Water Res. 262, 122119. <https://doi.org/10.1016/j.watres.2024.122119>.
- Welker, M., Von Döhren, H., 2006. Cyanobacterial peptides - Nature’s own combinatorial biosynthesis. FEMS Microbiol. Rev. 30 (4), 530–563. <https://doi.org/10.1111/j.1574-6976.2006.00022.x>.
- Wolf-Gladrow, D.A., Zeebe, R.E., Klaas, C., Körtzinger, A., Dickson, A.G., 2007. Total alkalinity: the explicit conservative expression and its application to biogeochemical processes. Mar. Chem. 106, 287–300. <https://doi.org/10.1016/j.marchem.2007.01.006>.
- Zhang, C.C., Zhou, C.Z., Burnap, R.L., Peng, L., 2018. Carbon/Nitrogen metabolic balance: lessons from cyanobacteria. Trends Plant Sci. 23 (12), 1116–1130. <https://doi.org/10.1016/j.tplants.2018.09.008>.
- Zheng, B., Du, Y., Deng, Y., Zhao, T., Dong, P., Shi, J., Wu, Z., 2023. Colonial morphology weakens the response of different inorganic carbon uptake systems to CO₂ levels in *Microcystis* population. Harmful Algae 128, 102491. <https://doi.org/10.1016/j.hal.2023.102491>.
- Zilliges, Y., Kehr, J.C., Meissner, S., Ishida, K., Mikkat, S., Hagemann, M., Kaplan, A., Börner, T., Dittmann, E., 2011. The cyanobacterial hepatotoxin microcystin binds to proteins and increases the fitness of *Microcystis* under oxidative stress conditions. PLoS ONE 6 (3). <https://doi.org/10.1371/journal.pone.0017615>.
- Zurawell, R.W., Chen, H., Burke, J.M., Prepas, E.E., 2005. Hepatotoxic cyanobacteria: a review of the biological importance of microcystins in freshwater environments. J. Toxicol. Environ. Health - Part B: Crit. Rev. 8 (1), 1–37. <https://doi.org/10.1080/10937400590889412>.